

Synthesis, characterization, DNA-binding and biological activity of Zn(II) complexes of sulfadiazine with different amino acids

Ahmed Abdmonem El-Henawy ^{1,2} and Ahmed Imam Hanafy ^{2,3,*}

¹ Chemistry Department, Faculty of Science, Al-Baha University, Al-Baha, 1988, Saudi Arabia

² Chemistry Department, Faculty of Science, Al-Azhar University, Cairo, 11884, Egypt

³ Chemistry Department, Faculty of Science, Taif University, Taif, 21985, Saudi Arabia

* Corresponding author at: Chemistry Department, Faculty of Science, Al-Azhar University, Cairo, 11884, Egypt. Tel.: +96.612.8322143. Fax: +96.612.8322143. E-mail address: ahmedih@yahoo.com (A.I. Hanafy).

ARTICLE INFORMATION



DOI: 10.5155/eurjchem.6.2.117-126.1172

Received: 19 October 2014

Received in revised form: 12 January 2015

Accepted: 18 January 2015

Published online: 30 June 2015

Printed: 30 June 2015

KEYWORDS

Docking
 Antifungal
 Amino acid
 Sulfadiazine
 DNA-binding
 Antibacterial activity

ABSTRACT

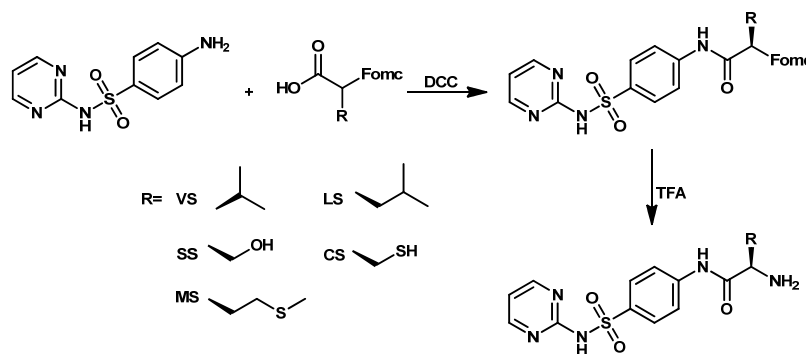
New Zn(II) complexes (Zn^{II}-VS, Zn^{II}-LS, Zn^{II}-SS, Zn^{II}-CS and Zn^{II}-MS) of the sulfonamide antibiotic sulfadiazine with different amino acids were prepared and fully characterized by elemental analyses, thermal analysis and IR, UV/Vis and ¹H NMR spectroscopy. The IR and ¹H NMR spectral data show that the ligands behave in a dibasic bidentate fashion coordinating to zinc ion. Interactions of these complexes with DNA were investigated by spectrophotometric method. Moreover, the antibacterial and antifungal activities were evaluated for five ligands and their complexes. The computational study for prediction of absorption, distribution, metabolism, elimination and toxic factors (ADMET) properties were performed for the prepared ligands.

Cite this: *Eur. J. Chem.* 2015, 6(2), 117-126

1. Introduction

In recent years, many researches have focused on exploring interaction of small molecules with DNA [1,2]. DNA is generally the primary intracellular target of anticancer drugs, so the interaction between small molecules and DNA can cause DNA damage in cancer cells, blocking the division of cancer cells, and resulting in cell death [3,4]. Drug-DNA interactions can be classified into two major categories, intercalation and groove binding. Intercalation involves the insertion of a planar molecule between DNA base pairs, which results in a decrease in the DNA helical twist and lengthening of DNA [5]. Groove binding, unlike intercalation, does not induce large conformational changes in DNA and may be considered similar to standard lock-and-key models for ligand-macromolecular binding [6]. Interestingly, the correlation between DNA-binding and cytotoxic activity against cancer cells is still a crucial step in the search for new anticancer drugs [7-10]. The only limitation to their application as drugs could stem from the lower thermodynamic and/or kinetic stability of their metal complexes used as drugs [11] compared with the analogous ruthenium(II) or platinum(II) partners [12]. However, this may be depending strongly on the nature

of the coordinating ligands. Among the metal ions regarded as coordination centers of potential anticancer agents, platinum and ruthenium ions are the most widely investigated up to now [13,14]. However, there is a growing interest in the synthesis of cheaper first-row transition metal complexes as efficient DNA binders with potential cytotoxic activity [15,16]. These metal ions are nowadays present in several inorganic pharmaceuticals used as drugs against a variety of diseases, ranging from antibacterial and antifungal to anticancer applications [17-19]. In the literature, diverse zinc complexes with biological activity are reported; among them zinc complexes with drugs used for the treatment of Alzheimer disease [20]. Other complexes showed antibacterial [21], antidiabetic [22], anti-inflammatory [23], antimicrobial [24] and antiproliferative-antitumor activities [25,26]. A number of zinc metal complexes have been synthesized and studied for their bioactivity [27,28]. Especially, binding of zinc(II) complexes to DNA has attracted much attention [29,30]. Nitrogen ligands have been extensively used in coordination chemistry [31,32], especially to obtain derivatives able to mimic structural, spectroscopic and catalytic features of active sites of metallo-enzymes [33,34].



Scheme 1

In this study, a series of Zn(II) complexes of sulfadiazine with different amino acid has been synthesized and characterized. The prepared complexes were used to investigate their ability to bind DNA and therefore, can be used as anticancer. In addition, the microbial activities of the prepared complexes were evaluated.

2. Experimental

2.1. Instrumentation

Carbon, hydrogen and nitrogen contents were determined at the Microanalytical Unit, Cairo University, Egypt. IR spectra of the ligands and their solid complexes were measured in KBr on a Mattson 5000 FT-IR spectrometer. All electronic spectra and kinetic measurement were performed using Varian Cary 4 Bio UV/Vis spectrophotometer. ^1H NMR spectra of the ligands and complexes were recorded on JEOL-90Q Fourier Transform (300 MHz) spectrometers in $\text{DMSO-}d_6$. The mass spectrum of the ligand was recorded on a Shimadzu GC-S-QP 1000 EX spectrometer using a direct inlet system. Thermal analysis measurements (TGA, DTA) were recorded on a Shimadzu thermogravimetric analyzer model TGA-50H, using 20 mg samples. The flow rate of nitrogen gas and heating rate were 20 cm^3/min and 10 $^\circ\text{C}/\text{min}$, respectively.

2.2. Materials and methods

Sulfadiazine, DL-Methionine, L- Cystine, DL-Valine, DL-leucine, DL-Serine, *N,N'*-dicyclohexyl carbodiimide, zinc chloride, 9*H*-fluoren-9-ylmethoxycarbonyl (Fmoc) and DNA (Calf thymus type I, Sigma) were purchased from Sigma-Aldrich.

2.3. Synthesis of organic ligands

A mixture of sulfadiazine (0.01 mole) and 0.01 mole of Fmoc-amino acid was dissolved in 40 mL tetrahydrofuran (Scheme 1). The mixture was cooled to 0 $^\circ\text{C}$, then 2.06 g (0.01 mole) *N,N'*-dicyclohexyl carbodiimide (DCCD) dissolved in 10 mL tetra-hydrofuran was added. The reaction mixture was stirred for 3-5 h at 0 $^\circ\text{C}$, then allowed to stand for 24 h at room temperature. A few drops of acetic acid was added, then the precipitate of *N,N'*-dicyclohexylurea was filtered off. The filtrate was concentrated in vacuum to dryness. The residual material was recrystallized from ethanol-water, and obtained in 75-80 % yield. The amino acid-sulfadiazine ligands were chromatographically homogenous when developed with iodine solution-benzidine and gave negative ninhydrin test.

2-Amino-3-methyl-N-(4-(N-(pyrimidin-2-yl)sulfamoyl)phenyl)butanamide (VS): Yield: 79%. FT-IR (KBr, ν , cm^{-1}): 3340, 3200 (NH_2), 3038 (NH), 2934 (CH-Arom), 1640 (CO),

1587 (CN), 1496 (NH_2), 1442 (SO_2). ^1H NMR (300 MHz, $\text{DMSO-}d_6$, δ , ppm): 11.48 (b, s, 2H, NH_2), 8.45 (s, 1H, NH NHC(O)), 8.31 (s, 2H, 2CH-Pyrimidin), 7.62-6.50 (m, 5H, Ar-H (4H) + CH-Pyrimidin (1H)), 5.74 (s, 1H, NHSO_2), 3.33-2.40 (m, 8H, Aliphatic). Anal. calcd. for $\text{C}_{15}\text{H}_{19}\text{N}_5\text{O}_3\text{S}$: C, 51.56; H, 5.48; N, 20.07%. Found: C, 51.50; H, 5.40; N, 20.07%.

2-Amino-4-methyl-N-(4-(N-(pyrimidin-2-yl)sulfamoyl)phenyl)pentanamide (LS): Yield: 80%. FT-IR (KBr, ν , cm^{-1}): 3354, 3236 (NH_2), 3038 (NH), 2948 (CH-Arom), 1652 (CO), 1586 (CN), 1496 (NH_2), 1442 (SO_2). ^1H NMR (300 MHz, $\text{DMSO-}d_6$, δ , ppm): 10.56 (b, s, 2H, NH_2), 8.45 (s, 1H, NH NHC(O)), 8.31 (s, 2H, 2CH-pyrimidin), 7.64-6.45 (m, 5H, Ar-H (4H) + CH-pyrimidin (1H)), 5.05 (s, 1H, NHSO_2), 3.33-2.49 (m, 10H, Aliphatic). Anal. calcd. for $\text{C}_{16}\text{H}_{21}\text{N}_5\text{O}_3\text{S}$: C, 52.88; H, 5.82; N 19.27%. Found: C, 52.89; H, 5.84; N, 19.30%.

2-Amino-3-hydroxy-N-(4-(N-(pyrimidin-2-yl)sulfamoyl)phenyl)propanamide (SS): Yield: 78%. FT-IR (KBr, ν , cm^{-1}): 3354, 3244 (NH_2), 3038 (NH), 2936 (CH-Arom), 1648 (CO), 1587 (CN), 1496 (NH_2), 1442 (SO_2), 3500 (OH). ^1H NMR (300 MHz, $\text{DMSO-}d_6$, δ , ppm): 11.42 (b, s, 2H, NH_2), 8.47 (s, 1H, NH NHC(O)), 8.33 (s, 2H, 2CH-pyrimidin), 7.59-6.48 (m, 5H, Ar-H (4H) + CH-pyrimidin (1H)), 5.69 (s, 1H, NHSO_2), 4.62 (s, 1H, OH-Ser), 3.33 (bs, 1H, CH-Ser), 2.51 (s, 2H, CH_2 -Ser). Anal. calcd. for $\text{C}_{13}\text{H}_{15}\text{N}_5\text{O}_4\text{S}$: C, 46.28; H, 4.48; N, 20.76%. Found: C, 46.21; H, 4.56; N, 20.80%.

2-Amino-3-mercapto-N-(4-(N-(pyrimidin-2-yl)sulfamoyl)phenyl)propanamide (CS): Yield: 82%. FT-IR (KBr, ν , cm^{-1}): 3380, 3225 (NH_2), 3036 (NH), 2950 (CH-Arom), 1650 (CO), 1596 (CN), 1496 (NH_2), 1440 (SO_2), 2650 (SH). ^1H NMR (300 MHz, $\text{DMSO-}d_6$, δ , ppm): 11.26 (b, s, 2H, NH_2), 8.48 (s, 1H, NH NHC(O)), 8.37 (s, 2H, 2CH-pyrimidin), 7.96-6.55 (m, 5H, Ar-H (4H) + CH-pyrimidin (1H)), 6.00 (s, 1H, NHSO_2), 2.88 (s, 1H, CH-CS), 2.73 (s, 2H, CH_2 -CS), 2.08 (s, 1H, SH-CS). Anal. calcd. for $\text{C}_{13}\text{H}_{15}\text{N}_5\text{O}_3\text{S}_2$: C, 44.18; H, 4.28; N, 19.82%. Found: C, 44.15; H, 4.30; N, 19.84%.

2-Amino-4-(methylthio)-N-(4-(N-(pyrimidin-2-yl)sulfamoyl)phenyl)butanamide (MS): Yield: 85%. FT-IR (KBr, ν , cm^{-1}): 3348, 3256 (NH_2), 3086 (NH), 2936 (CH-Arom), 2872 (CH-Aliphatic), 1650 (CO), 1586 (CN), 1496 (NH_2), 1440 (SO_2). ^1H NMR (300 MHz, $\text{DMSO-}d_6$, δ , ppm): 11.11 (b, s, 2H, NH_2), 8.48 (s, 1H, NH NHC(O)), 8.37 (s, 2H, 2CH-pyrimidin), 7.96-6.59 (m, 5H, ArH (4H) + CH-pyrimidin (1H)), 5.99 (s, 1H, NHSO_2), 3.38-2.09 (m, 8H-Aliphatic protons). Anal. calcd. for $\text{C}_{15}\text{H}_{19}\text{N}_5\text{O}_3\text{S}_2$: C, 47.23; H, 5.02; N, 18.36%. Found: C, 47.29; H, 5.04; N, 18.40%.

2.4. Synthesis of zinc complexes

Zinc (II) chloride (0.01 mole) was dissolved in 40 mL ethanol, then added to 0.01 mole of the prepared ligand dissolved in 40 mL ethanol. The mixture was heated under reflux for 2 h.

Table 1. Pharmacokinetic parameters important for good oral bioavailability of all ligands *.

Compound	TPSA	%ABS	CLogP	LogS	MW	nON	nOHNH	Lip-V.	Volume A ³	E gap.	Mr	$[\alpha]_D^{20}$
L-VS	127.07	65.16	0.04	-2.56	349.42	8	4	0	300.43	-8.65	90.79	+33.5
L-LS	127.07	65.16	0.57	-4.00	363.44	8	4	0	317.23	-8.71	101.46	+38
L-SS	147.30	58.18	-0.74	-2.24	337.36	9	5	0	275.29	-8.75	89.09	+20
L-CS	127.07	65.16	0.75	-3.43	353.42	8	4	0	284.94	-8.87	95.57	+28
L-MS	127.07	65.16	0.28	-3.64	381.48	8	4	0	318.77	-8.18	105.01	+42

* TPSA: Total Polar surface area, %ABS: 109-0.345 * TPSA, C Log P: Calculated lipophilicity, Log S: Solubility parameter, nON: Number of hydrogen bond acceptor, nOHNH: Number of hydrogen bond donor, Lip-V: Number of violation from Lipinski's rule of five, Mr: Molar Refractivity, $[\alpha]_D^{20}$: Optical rotations (c=0.1, MeOH).

The precipitate was formed, filtered off and finally washed by hot ethanol several times and dried in an open air.

Zn^{II}-VS, Zn(VS)(OH)₂.2H₂O: Yield: 75%. FT-IR (KBr, v, cm⁻¹): 3352, 3250 (NH₂), 3038 (NH), 2940 (CH-Arom), 1650 (CO), 1586 (CN), 1490 (NH₂), 1442 (SO₂). ¹H NMR (300 MHz, DMSO-*d*₆, δ, ppm): 11.50 (b, s, 2H, NH₂), 8.48 (s, 1H, NH NHCO), 8.33 (s, 2H, 2CH-pyrimidin), 7.60-6.49 (m, 5H, ArH (4H) + CH-pyrimidin (1H)), 5.74 (s, 1H, NHSO₂), 3.33-2.40 (m, 8H, Aliphatic protons). Anal. calcd. for C₁₅H₂₅N₅O₇SZn: C, 37.16; H, 5.16; N, 14.45. Found: C, 37.10; H, 5.20; N, 14.41%.

Zn^{II}-LS, Zn(LS)(OH)₂.H₂O: Yield: 75%. FT-IR (KBr, v, cm⁻¹): 3342, 3254 (NH₂), 3038 (NH), 2942 (CH-Arom), 1635 (CO), 1588 (CN), 1490 (NH₂), 1440 (SO₂). ¹H NMR (300 MHz, DMSO-*d*₆, δ, ppm): 10.56 (b, s, 2H, NH₂), 8.47 (s, 1H, NH NHCO), 8.30 (s, 2H, 2CH-pyrimidin), 7.70-6.47 (m, 5H, ArH (4H) + CH-pyrimidin (1H)), 5.05 (s, 1H, NHSO₂), 3.33-2.49 (m, 10H, Aliphatic protons). Anal. calcd. for C₁₆H₂₅N₅O₆S₂Zn: C, 39.96; H, 5.20; N, 14.57. Found: C, 40.00; H, 5.23; N, 14.59%.

Zn^{II}-SS, Zn(SS-H)(OH)₂.0.5H₂O: Yield: 73%. FT-IR (KBr, v, cm⁻¹): 3354, 3244 (NH₂), 3038 (NH), 2942 (CH-Arom), 1658 (CO), 1584 (CN), 1490 (NH₂), 1442 (SO₂). ¹H NMR (300 MHz, DMSO-*d*₆, δ, ppm): 11.50 (b, s, 2H, NH₂), 8.48 (s, 1H, NH NHCO), 8.32 (s, 2H, 2CH-pyrimidin), 7.59-6.48 (m, 5H, ArH (4H) + CH-pyrimidin (1H)), 5.69 (s, 1H, NHSO₂), 3.33 (b, s, 1H, CH-Ser), 2.51 (s, 2H, CH₂-Ser). Anal. calcd. for C₁₃H₁₇N₅O_{6.5}SZn: C, 36.59; H, 4.35; N, 15.23. Found: C, 36.58; H, 4.35; N, 15.22%.

Zn^{II}-CS, Zn(CS-H)₂.H₂O: Yield: 77%. FT-IR (KBr, v, cm⁻¹): 3350, 3262 (NH₂), 3038 (NH), 2944 (CH-Arom), 1650 (CO), 1586 (CN), 1490 (NH₂), 1440 (SO₂). ¹H NMR (300 MHz, DMSO-*d*₆, δ, ppm): 11.38 (b, s, 4H, NH₂), 8.49 (s, 2H, NH NHCO), 8.40 (s, 4H, 2CH-pyrimidin), 7.61-6.51 (m, 10H, ArH (8H) + CH-pyrimidin (2H)), 5.93 (s, 2H, NHSO₂), 2.78 (s, 2H, CH-CS), 2.66 (s, 4H, CH₂-CS). Anal. calcd. for C₂₆H₃₀N₁₀O₇S₄Zn: C, 39.62; H, 3.81; N, 17.78. Found: C, 39.66; H, 3.84; N, 17.76%.

Zn^{II}-MS, Zn(MS)(OH)₂.H₂O: Yield: 79%. FT-IR (KBr, v, cm⁻¹): 3314, 3266 (NH₂), 3088 (NH), 2936 (CH-Arom), 2872 (CH-Aliphatic), 1638 (CO), 1586 (CN), 1490 (NH₂) 1442 (SO₂). ¹H NMR (300 MHz, DMSO-*d*₆, δ, ppm): 11.40 (b, s, 2H, NH₂), 8.48 (s, 1H, NH NHCO), 8.37 (s, 2H, 2CH-pyrimidin), 7.61-6.50 (m, 5H, ArH (4H) + CH-pyrimidin (1H)), 5.89 (s, 1H, NHSO₂), 3.42-2.50 (m, 8H, Aliphatic protons). Anal. calcd. for C₁₅H₂₃N₅O₆S₂Zn: C, 36.11; H, 4.61; N, 14.04. Found: C, 36.33; H, 4.64; N, 14.08%.

2.5. Biological screening

2.5.1. Evaluation of the degree of DNA binding

2.5.1.1. DNA binding assay on TLC plates

A fixed amount of the ligand (5 mg/mL in methanol) is spotted on the RP-18 TLC plates [35], followed by addition of known amount of DNA (1 mg/mL in methanol:water mixture (8:2, v:v)) on the same spot. Daunomycin was used as a positive control. After complete spotting, the plates were developed with the same solvent system. The position of unbound DNA was visualized by spraying the plates with anisaldehyde which produces a blue color with DNA. The

intensity of the color was proportional to the quantity of DNA added to the plate.

2.5.1.2. Colorimetric assay for the degree of DNA binding

DNA/methyl green complex (20 mg) was suspended in 100 mL of 0.05 M *tris*-HCl buffer (pH = 7.5) containing 7.5 mM MgSO₄ and stirred at 37 °C with a magnetic stirrer for 24 h [36]. The calculated amounts of samples were placed in Eppendorf tubes. Then, 200 μL of the DNA-methyl green solution was added to each tube. The samples were incubated in dark at room temperature, for 24 h. The final absorbance of each sample was determined at 642-645 nm. The results were recorded in form of the IC₅₀ for each compound. IC₅₀ means the sample concentration required to produce 50% decrease in the initial absorbance of the DNA-methyl green complex.

2.5.2. Anti-microbial screening

The anti-bacterial activity of the synthesized compounds was tested against two Gram-negative bacteria: *Escherichia coli* (NCTC 10416), *Pseudomonas aeruginosa* (NCIB 9016), and two Gram-positive bacteria: *Bacillus subtilis* (NCIB 3610), *Staphylococcus aureus* (NCTC 7447), and fungi namely *Candida albicans* (IMRU 3669) and *Aspergillus fumigatus* (ATCC-22019) using nutrient agar medium.

2.5.2.1. Paper disc diffusion technique

The synthesized L-amino acids sulfadiazine ligands and their corresponding complexes were tested for their *in vitro* antibacterial activity by using paper disc diffusion technique [37,38]. The sterilized (autoclaved at 120 °C for 30 min) medium (40-50 °C) was incubated (1 mL/100 mL of medium) with the suspension (10⁵ cfu/mL) of the micro-organism (matched to McFarland barium sulphate standard) and poured into a petridish to give a depth of 3-4 mm. The paper impregnated with the tested compounds (μg/mL in methanol) was placed on the solidified medium. The plates were pre-incubated for 1 h at room temperature and incubated at 37 °C for 24 and 48 h for anti-bacterial and anti-fungal activities, respectively. Ampicillin (mg/disc) was used as a standard for antibacterial and anti-fungal activity, respectively. The observed zones of inhibition are presented in (Table 1).

2.5.2.2. Minimum inhibitory concentration (MIC)

Minimum inhibitory concentration (MIC) of the compound was determined by agar streak dilution method. A stock solution of the synthesized compound (100 μg/mL) in dimethyl formamide was prepared and graded quantities of the tested compounds were incorporated in specified quantity of molten sterile agar (nutrient agar for anti-bacterial activity and sabouraud dextrose agar medium for anti-fungal activity). A specified quantity of the medium (40-50 °C) containing the compound was poured into a petridish to give a depth of 3-4 mm and allowed to solidify. Suspension of the micro-organism was prepared to contain approximately (10⁵ cfu/mL) and

applied to plates with serially diluted compounds in dimethyl formamide to be tested and incubated at 37 °C for 24 and 48 h for bacteria and fungi, respectively. The MIC was considered to be the lowest concentration of the test substance exhibiting no visible growth of bacteria or fungi on the plate.

2.6. Molecular modeling

The structural model was built using the BUILDER module of Molecular Operating Environment (MOE). Optimization Conformational analyses of the built molecules were performed in a two-step procedure. First, these compounds were submitted to energy minimization tool using the included MOPAC 7.0. The geometry of the compounds was optimized using the semi-empirical AM1 Hamiltonian with Restricted Hartree-Fock (RHF) and RMS gradient of 0.05 Kcal/mol. Then, the obtained model was implemented to the 'Systematic Conformational Search' of the MOE. All items were set as default with RMS gradient of 0.01 Kcal/mol and RMS distance of 0.1 Å. The obtained data were then output into a MDB file to be used in the DOCKING calculations.

2.7. Docking calculations

The crystal structure of the [d(CGCAATTTGCG)]₂ with a distamycin molecule was used for the receptor molecule, water and distamycin molecules around the duplex were removed, then hydrogen atoms were added. The parameters and charges were assigned with MMFF94x force field. After alpha-site spheres were generated using the SITE FINDER module of MOE, the structural model of complexes were docked on the surface of the interior of the minor groove using the DOCK module of MOE.

3. Results and discussion

3.1. IR and ¹H NMR spectroscopy of the organic ligands

The organic ligands have been prepared using (Fmoc) as a protective group. Fmoc group is generally removed from the N terminus of a peptide chain by acidolysis using trifluoroacetic acid (TFA) [39]. The organic ligands DL-methionionyl sulfadiazine (MS) and L-cystinoyl sulfadiazine (CS) have been prepared and characterized earlier [40]. The IR spectral data of VS, SS and LS show two bands at 3340-3354 and 3200-3244 cm⁻¹ attributed to νNH₂. The IR spectra also show band at 1640-1652 cm⁻¹ corresponding to νCO, at the same time the band attributed to ν(O=S=O) is appearing around 1440 cm⁻¹ [41,42]. The band at 3500 cm⁻¹ in the SS spectrum is corresponding to νOH. ¹H NMR spectra of CS and SS ligands in dimethyl-sulfoxide-*d*₆ exhibited signals at δ 11.26 and 11.42 ppm, respectively, assigned to 2H, NH₂. L-Cystinoyl sulfadiazine shows a signal at δ 2.08 ppm assigned to 1H, SH, whereas the spectrum of DL-Serinoyl sulfadiazine, (SS) shows a signal at δ 4.62 ppm assigned to 1H, OH. The mass spectroscopy shows molecular ion peak at 381, 353, 349, 351 and 363 for MS, CS, VS, SS and LS, respectively. The IR, ¹H NMR and mass spectroscopy together with %C, %H and %N mentioned earlier suggest the proposed structure of the ligands under investigation as shown in Scheme 1.

3.2. IR and ¹H NMR spectroscopy of zinc(II) complexes

In order to investigate the mode of binding of zinc ion to the organic ligands, the IR spectral data of the prepared ligands were compared to that of the zinc complexes. In case of Zn(II) complexes of MS, VS and LS ligands, the mode of binding was found to be coordination of the ligands to the zinc ion through carbonyl oxygen and nitrogen atom of the NH₂ group. This assumption was supported by the observed IR spectral data. The bands attributed to ν(NH₂) in the IR spectra of the

Zn(II) complexes were shifted to 3314-3352 and 3200-3266 cm⁻¹. The carbonyl band ν(C=O) which appears at 1640-1652 cm⁻¹ in ligands spectra was shifted to lower wavenumber with smaller intensities than that of the free ligands. The bands assigned to ν(O=S=O), ν(CN) and ν(NH) appear at the same position in the Zn(II) complexes spectra with no change representing no participation in the coordination. The IR spectral data for Zn^{II}-CS represents that the Zn ion binds to CS through SH group with displacement of its proton and NH₂ nitrogen atom. This mode of binding is supported by disappearance of the band assignable to SH in the Zn^{II}-CS spectrum with shifting of the bands attributed to amino group to 3350 and 3262 cm⁻¹. This assumption also was supported by disappearing the signal at δ 2.08 ppm assigned to 1H, SH in the ¹H NMR spectrum of the Zn^{II}-CS. At the same time, by comparing the IR spectral data of SS with its Zn(II) complex, one can observe that the band corresponding to carbonyl ν(C=O) was shifted to 1658 cm⁻¹ in the Zn^{II}-SS. The OH band in the spectrum of the complex is obscured. The ¹H NMR spectrum of Zn^{II}-SS reveals the disappearance of the signal at δ 4.62 ppm assigned to 1H, OH. These data suggest that the Zn(II) ion binds to SS through carbonyl oxygen atom and OH with displacement of its proton. The position of ν(NH), ν(O=S=O) and ν(NH₂) bands in the Zn^{II}-CS and Zn^{II}-SS complexes spectra indicate that these functional groups do not participate in the coordination. The IR spectra for all complexes show a broad band at ~3450 cm⁻¹ assigned to ν(OH) stretching vibration of water molecule and OH group in the all synthesized complexes.

3.3. Electronic spectroscopy

Since the zinc ion has *d*¹⁰ configuration, no *d-d* transition are expected for Zn(II) complexes [43]. The electronic spectra of all Zn(II) complexes under investigation dissolved in DMSO show absorption bands at 227-420 nm which can be assigned to charge transfer from the ligand to the metal and vice versa. Based on the diamagnetic character and these observed bands, a tetrahedral geometry [44,45] could be assumed for all Zn(II) complexes.

3.4. Thermal analysis

The TGA thermogram confirms the amount of solvent inside and/or outside the coordination sphere and gives some information about the stability of the compound. The correlations between the different decomposition steps of the complexes with the corresponding weight losses are discussed in terms of the proposed formula of the complexes as follow.

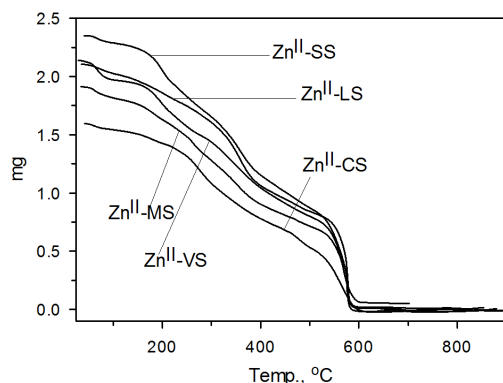
The thermogram TGA of all complexes in this study (Figure 1) shows 4-5 stages of mass loss in the temperature range of 25-800 °C. The first stage in the temperature range of 29-98 °C corresponds to removal of (0.5-2.0) water molecule with weight loss (calc. = 2.0-7.7%, found = 1.9-6.9%). The second peak in the temperature range of 90.7-300.9 °C corresponds to removal of CO₂, (NH₃ + CO₂), (NH₃ + 2CO₂), NH₃ and (NH₃ + CO₂ + H₂O + CH₃OH) molecules for Zn^{II}-MS, Zn^{II}-CS, Zn^{II}-VS, Zn^{II}-LS and Zn^{II}-SS, respectively. This inflection stages are accompanied with weight loss (calc. = 8.8, 7.7, 21.6, 9.1 and 25.1%, found = 8.8, 6.7, 20.6, 9.1 and 24.6%) for Zn^{II}-MS, Zn^{II}-CS, Zn^{II}-VS, Zn^{II}-LS and Zn^{II}-SS, respectively. The third and fourth stages are corresponding to degradation of the rest of the complexes leaving Zn oxides or carbides at the final stage.

The thermodynamics activation parameters of the decomposition process were evaluated using the well-known Coats-Redfern equation [46] in the form:

$$\ln \left[\frac{-\ln(1-\alpha)}{T^2} \right] = -\frac{E}{RT} + \ln \frac{AR}{\beta E} \quad (1)$$

Table 2. Thermodynamic parameters for all synthesized complexes.

Complex	First inflection point / Last inflection point		ΔS (J/Kmol)	ΔG (kJ/mol)
	E (kJ/mol)	ΔH (kJ/mol)		
Zn ^{II} -CS	9.60 / 10.9	6.82 / 4.02	-21.37 / -38.73	13.96 / 36.40
Zn ^{II} -MS	73.03 / 99.03	70.26 / 92.87	-9.91 / -33.05	73.57 / 119.71
Zn ^{II} -SS	40.70 / 134.31	37.87 / 127.27	-35.15 / -37.31	49.82 / 158.87
Zn ^{II} -VS	3.28 / 131.	2.45 / 124.08	-35.76 / -36.92	12.61 / 155.36
Zn ^{II} -LS	16.87 / 122.	14.01 / 115.34	-36.12 / -22.87	26.44 / 134.71

**Figure 1.** TGA for all synthesized complexes.

where α is the fraction of decomposition, R is the universal gas constant, E is the activation energy, A is constant and β is the heating rate. Therefore, plotting $\ln \left[\frac{-\ln(1-\alpha)}{T^2} \right]$ against $1/T$

according to equation (1) gives a straight line whose slope is directly proportional to the activation energy ($-E/R$). The activation entropy ΔS , the activation enthalpy ΔH , and the free energy (Gibbs function, ΔG) were calculated (Table 2) using the following equations [47]:

$$\Delta S = 2.303 \cdot \left(\log \frac{A \cdot h}{k \cdot T} \right) \cdot R \quad (2)$$

$$\Delta H = E - RT \quad (3)$$

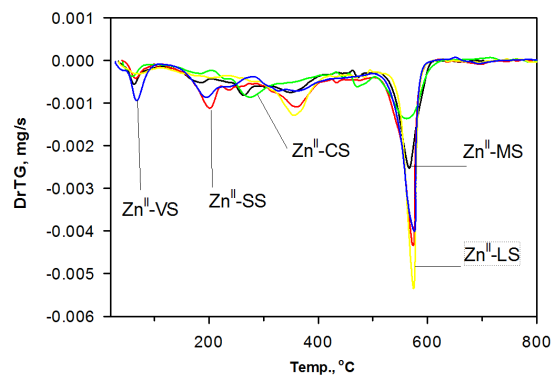
$$\Delta G = \Delta H - T \Delta S \quad (4)$$

where k and h are Boltzmann's and Planck's constants, respectively, T is the temperature involved in the calculation and selected as the peak temperature of Dr-TGA (Figure 2). The thermodynamic parameters for the first and last inflection points were calculated and listed in Table 2. The activation energies of decomposition were found to be in the range of 3.28-73.03 and 10.97-134.31 kJ/mol for first and last inflection stages, respectively. The high values of the activation energies for Zn^{II}-SS, Zn^{II}-VS and Zn^{II}-LS reflect the thermal stability of these complexes [48]. The entropy ΔS gives information about the degree of disorder of the system. The entropy of activation was found to have negative values in all the complexes which indicate that the decomposition reactions proceed with a lower rate than the normal ones and also, indicate that the complexes are formed spontaneously [48,49]. The enthalpy ΔH gives information about the total thermal motion and Gibbs or free energy gives information about the stability of the system.

The IR, electronic and ¹H NMR spectroscopy together with the thermal and elemental analysis data suggest the proposed structures for Zn(II) complexes as shown in the experimental section. The proposed structures for all complexes are

represented as Zn(VS)(OH)₂ · 2H₂O, Zn(LS)(OH)₂ · H₂O, Zn(SS-H)(OH)₂ · 0.5H₂O, Zn(CS-H)₂H₂O and Zn(MS)(OH)₂ · H₂O.

In order to establish enantiomeric purity of isolated compounds, specific rotation values $[\alpha]_D^{20}$ were determined, and found to be remained unchanged after repeated crystallization for several times. Also, enantiomeric excess (ee) and diastereoisomeric excess (de) values were determined for the prepared ligands and compared with the values of the free amino acids. These values with the HPLC analytical data revealed that the optical purity of the resulting compounds was greater than 98%. Thus, as expected, stereochemical configuration at α -carbon atom of the amino acid was practically unaffected and this synthetic transformation from chiral α -amino acid could be applied to a wide range of compounds without undergoing any significant loss of optical activity.

**Figure 2.** Dr-TGA for all synthesized complexes Blue = VS, Yellow = LS, Red = SS, Green = CS, Black = MS.

3.5. Biological screening

3.5.1. DNA as an affinity probe for evaluation of biologically active compounds

3.5.1.1. DNA Binding assay

The small molecules binding with DNA has attracted attention in the medicinal design of anticancer and/or anti-AIDS drugs [50,51]. Both of TLC plates and colorimetric methyl green-DNA displacement assay are employed to determine the binding characteristics of metal complex with DNA. In the TLC plate method, after developing the plate, the position of unbound DNA was determined by spraying the plates with anisaldehyde reagent. It was demonstrated that, when DNA was mixed with compounds known to interact with it, e.g. ethidium bromide, the complex was retained at the origin. Compounds with high binding affinity to DNA remained on the base line or migrated for a very short distance, while compounds with poor binding affinity did not cause DNA to be retained at the origin.

Methyl green reversibly binds with polymerized DNA, which forming a stable complex at neutral pH [36]. The maximum absorption for the DNA-methyl green complex is 642-645 nm.

Table 3. DNA binding activity of the synthesized L-aminoacid metal-complexes using methyl green DNA displacements assay, the values of energies calculated.

Compound	IC ₅₀ ^a	E Scor ^b	E ^c	E-ele ^d	HF ^e	HOMO ^f	LUMO ^g
Zn ^{II} -VS	56	-14.30	-127878.53	-950772.63	-109.53	-3.12	2.19
Zn ^{II} -LS	55	-4.11	-120459.95	-872885.19	-39.96	-0.02	3.68
Zn ^{II} -SS	10	-16.86	-116815.42	-769649.5	-121.39	-9.72	-0.86
Zn ^{II} -CS	13	-18.83	-196218.89	-1753947.1	89.76	2.15	7.91
Zn ^{II} -MS	19	-16.50	-121399.88	-881978.06	-66.22	-0.58	4.55
Dau.	29						
Compound	E.Gap ^h	Dipole ^k	IP ^l	E ^m	E ele ⁿ	E vdw ^p	
Zn ^{II} -VS	-5.32	8.00	9.72	-153.02	-347.29	127.72	
Zn ^{II} -LS	-3.71	15.71	0.02	-99.22	-218.81	45.92	
Zn ^{II} -SS	-8.85	9.12	2.25	-60.17	-169.26	53.39	
Zn ^{II} -CS	-5.75	10.27	-2.15	66.53	-64.57	79.29	
Zn ^{II} -MS	-5.14	14.58	0.58	-172.35	-365.40	100.85	
Dau.							

a = IC₅₀ (µg/mL) obtained from three independent determinations required for 50% decrease in the initial absorbance of DNA-methyl green solution,

b = Scoring binding free energy for best pose (kcal/mol).

c = The total energy (kcal/mol).

d = Electronic energy (kcal/mol).

e = Heat of formation (kcal/mol).

f = Highest Occupied Molecular Orbital (eV).

g = Lowest Occupied Molecular Orbital (eV).

h = Energy Gap (eV).

k = Dipole moment calculated.

l = Ionization potential.

m = Potential energy.

n = Electrostatic energy.

p = Vander Waals energy.

Table 4. Anti-microbial activity of the synthesized compounds *.

Compound	In-vitro activity-zone of inhibition in mm (MIC in µg/mL)											
	<i>E. coli</i>		<i>B. subtilis</i>		<i>S. aureus</i>		<i>P. aeruginosa</i>		<i>C. albicans</i>		<i>A. fumigatus</i>	
	A	MIC	A	MIC	A	MIC	A	MIC	A	MIC	A	MIC
VS	17	-	5	-	5	-	5	-	5	-	5	-
LS	5	-	5	-	5	-	5	-	5	-	5	-
SS	18	5	15	5	10	5	17	5	19	5	15	5
CS	16	2.5	14	5	19	5	18	5	15	5	15	5
MS	5	-	5	-	5	-	5	-	5	-	5	-
Zn ^{II} -VS	18	2.5	14	5	17	2.5	28	2.5	21	2.5	27	2.5
Zn ^{II} -LS	20	5	20	5	19	5	25	1.25	18	2.5	24	5
Zn ^{II} -SS	23	1.25	18	2.5	20	1.25	21	5	15	5	21	1.25
Zn ^{II} -CS	20	2.5	19	1.25	22	1.25	22	5	19	5	24	1.25
Zn ^{II} -MS	16	5	13	5	10	5	14	5	15	2.5	14	2.5
Ampicillin	29	5	31	2.5	30	1.25	29	1.25	4	-	5	-
Chloroform	-	-	-	-	-	-	-	-	-	-	-	-

* (-) Inactive (8 mm), weak activity (8-14 mm), moderate activity (14-20 mm), strong activity (>20).

This colorimetric assay was used to measure the displacement of methyl green from DNA by compounds that having the ability to bind with DNA. The degree of displacement was determined spectrophotometrically by measuring the change in the initial absorbance of the DNA-methyl green solution in the presence of reference compound. Results from DNA binding assay (Table 3) revealed that the complexes Zn^{II}-SS, Zn^{II}-CS and Zn^{II}-MS showed the highest affinity (IC₅₀ = 10, 13 and 19 µg/mL, respectively). These data have been supported by retaining the complexes at the origin or by migrating for very short distances. This high affinity may be due to the presence of the polarity nature of the amino acid residues which increase the bonding interaction with DNA. The other two complexes Zn^{II}-VS and Zn^{II}-LS showed moderate IC₅₀ (55 and 56, µg/mL).

3.5.2. Antimicrobial activity

3.5.2.1. Antibacterial activity

The tested micro-organism strains used in this study are Gram-negative bacteria: *Escherichia coli* (NCTC-10416), *Pseudomonas aeruginosa* NCIB9016 and Gram-positive bacteria *Bacillus subtilis* (NCIB-3610), *Staphylococcus aureus* (NCTC-7447). Ampicillin was used as standard drug. The results of antimicrobial activity taken as inhibition zone diameter and minimum inhibitory concentration (MIC) were furnished in Table 4. From Table 4, it's clearly that the ligands SS and CS were found to be low to moderate active against all the tested bacterial strains with MIC 5 µg/mL. On the other

hand the ligands VS, LS and MS show no activity against tested bacterial strains. The ligand VS have moderate potency against *E. coli*. The complexes Zn^{II}-SS and Zn^{II}-CS have high potency against all the tested bacterial strains with MIC between 1.25 and 2.5 µg/mL except that of *B. subtilis* which has been affected moderately by these two complexes. Furthermore Zn^{II}-VS, Zn^{II}-LS and Zn^{II}-MS showed moderate to low activities (MIC = 2.5 and 5 µg/mL) against all tested bacterial strain. The complexes Zn^{II}-VS and Zn^{II}-LS have high activities against *P. aeruginosa* (MIC = 2.5 and 1.25 µg/mL), respectively.

3.5.2.2. Antifungal activity

In vitro antifungal studies of all synthesized ligands and their complexes were tested against *Candida albicans* (IMRU-3669) and *Aspergillus fumigatus* (ATCC-22019), Ampicillin was used as reference drug and their inhibition zone diameter and minimum inhibitory concentration (MIC) values were depicted in Table 4. In general, the synthesized L-amino acid ligands VS, LS and MS exerted inactive *in vitro* antifungal activity against all tested organisms. The ligands SS and CS showed moderate activities with MIC (5 µg/mL). Moreover, the complexes Zn^{II}-VS, Zn^{II}-LS, Zn^{II}-SS and Zn^{II}-CS showed high activities against *A. fumigatus* with MIC (1.25-5.00 µg/mL), while the complex Zn^{II}-MS shows low potency, MIC (5 µg/mL) with the same organism. Complexes Zn^{II}-LS, Zn^{II}-SS, Zn^{II}-CS and Zn^{II}-MS have moderate activity against *C. albicans* with MIC values (2.5 and 5.0 µg/mL). At the same time, the complex Zn^{II}-VS exerted high potency toward *C. albicans* with MIC (2.5 µg/mL).

Table 5. Calculated energies of L and D stereo isomer forms of all ligands.

Compound	E^a	$E^{ele\ b}$	HF^c	$HOMO^d$	$LUMO^e$	$Dipol^e$	IP^g	E^h	$E^{ele\ k}$	$E^{vdw\ l}$
D-VS	-100805.65	-698814.44	-29.63	-9.45	-0.74	3.83	9.70	12.08	-54.71	43.26
L-VS	-100807.79	-718525.81	-31.67	-9.52	-0.87	6.64	9.57	5.96	-59.14	40.15
D-LS	-104403.41	-742566	-40.67	-9.38	-0.65	7.51	9.38	-0.88	-59.85	45.32
L-LS	-104403.61	-758480	-40.87	-9.34	-0.63	9.18	9.34	-4.44	-61.77	45.43
D-SS	-98109.52	-640661.44	-19.08	-9.43	-0.76	7.34	9.54	-2.34	-54.27	42.03
L-SS	-101023.38	-661686.44	-72.45	-9.57	-0.82	6.29	9.43	-0.59	-57.48	40.77
D-CS	-98107.26	-658230.81	-17.05	-9.54	-0.93	5.08	9.45	0.28	-47.03	42.08
L-CS	-101024.77	-665777.75	-71.98	-9.70	-0.83	7.44	9.52	4.43	-50.20	40.47
D-MS	-105287.09	-723316	-23.29	-8.68	-0.67	7.26	8.98	2.71	-52.87	42.06
L-MS	-105294.09	-741711.94	-30.29	-8.98	-0.80	8.32	8.67	-1.49	-53.89	41.96

a = The total energy (kcal/mol).

b = Electronic energy (kcal/mol).

c = Heat of formation (kcal/mol).

d = Highest Occupied Molecular Orbital (eV).

e = Lowest Occupied Molecular Orbital (eV).

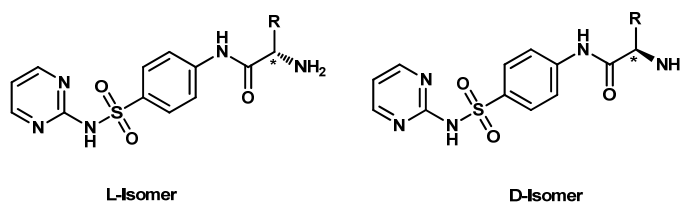
f = Dipole moment calculated.

g = Ionization potential.

h = Potential energy.

k = Electrostatic energy.

l = Van der Waals energy.

**Figure 3.** L- and D-forms of synthesized ligands.

3.6. Molecular modeling studies

3.6.1. ADMET factors profiling

Oral bioavailability was considered playing an important role for the development of bioactive molecules as therapeutic agents. Many potential therapeutic agents fail to reach the clinic because of ADMET (absorption, distribution, metabolism, elimination and toxic) factors. Therefore, a computational study for prediction of ADMET properties of the molecules was performed for the prepared ligands, by determination of topological polar surface area (TPSA), a calculated percent absorption (%ABS) which was estimated by Zhao *et al.* equation [52], and "rule of five", which have been formulated by Lipinski [53]. The "rule of five" established that the chemical compound could be developed to be a drug, if no more than one violation of the following rule:

- i. $C \log P$ (partition coefficient between water and octanol) < 5 ,
- ii. Number of hydrogen bond donors sites ≤ 5 ,
- iii. Number of hydrogen bond acceptors sites ≤ 10 ,
- iv. Molecular weight < 500 and molar refractivity should be between 40-130.

In addition, the total polar surface area (TPSA) is another key property linked to drug bioavailability; the passively absorbed molecules with (TPSA > 140) have low oral bioavailability [54]. All calculation descriptors were performed using MOE program [55], the results were disclosed in Table 1. Our results revealed that, the $C \log P$ (factor of the lipophilicity [56]) less than 5.0, the molecular weight (MW < 500), hydrogen bond acceptors between 8 and 9, hydrogen bond donors (4 and 5) and molar refractivity values approximately between 90 and 105 which fulfill Lipinski's rule. Also, the percent absorption of the whole synthesized ligands ranged between 58.1 and 65.1%. These data may suggest that the ligands VS, LS, SS, CS and MS have good oral absorption as antimicrobial compounds.

3.6.2. Conformational analysis

In trying to achieve better insight into the molecular structure of the most preferentially stereoisomer forms (L and/or D) and complexes, conformational analysis of the target compounds has been performed using the MMFF94 force-field [57,58] (calculations in vacuum, bond dipole option for electrostatics, Polake Ribiere algorithm, RMS gradient of 0.01 kcal/mol) implemented in MOE. The most stable conformer was fully geometrical optimized by AM1 [59] semi-empirical Hamiltonian molecular orbital calculation MOPAC package. Furthermore, the computed molecular parameters, total energy, binding energy, heat of formation, the lowest occupied molecular orbital (LUMO) and the highest occupied molecular orbital (HOMO) energies, potential energies, solvation energies, Electrostatic energies, van der Waals energy and the dipole moment for studied compounds were calculated (Table 3 and 5). It is obvious that, there is a possibility of existence the prepared ligand in both diastereoisomer forms (Figure 3). The calculated molecular parameters have been used to investigate the most stable isomer forms of the prepared amino acid ligands. The most stable isomer is found to be the L form (table 4). The results obtained from the enhancement of the computed energies of L-molecular skeleton form and the optical purity of the ligands, are leading us to neglect the D-Form. The calculation results showed that, the lowest minimization energy structures of the L-form ligands exhibited a common arrangement of the diazine ring to be coplanar with the phenyl ring in case of VS, LS and CS, and to be perpendicular with the phenyl ring in case of SS and MS (Figure 4). The diazine ring in the Zn(II) complexes was found to be at 45° with the phenyl ring (Zn^{II}-VS and Zn^{II}-SS) and parallel to the phenyl ring in case of Zn^{II}-LS, Zn^{II}-CS and Zn^{II}-MS (Figure 5).

The HOMO and LUMO of a molecule play important roles in intermolecular interactions [59] between the HOMO of the drug with the LUMO of the receptor and vice versa. The interactions were stabilized inversely with energy gap between the interacting orbitals.

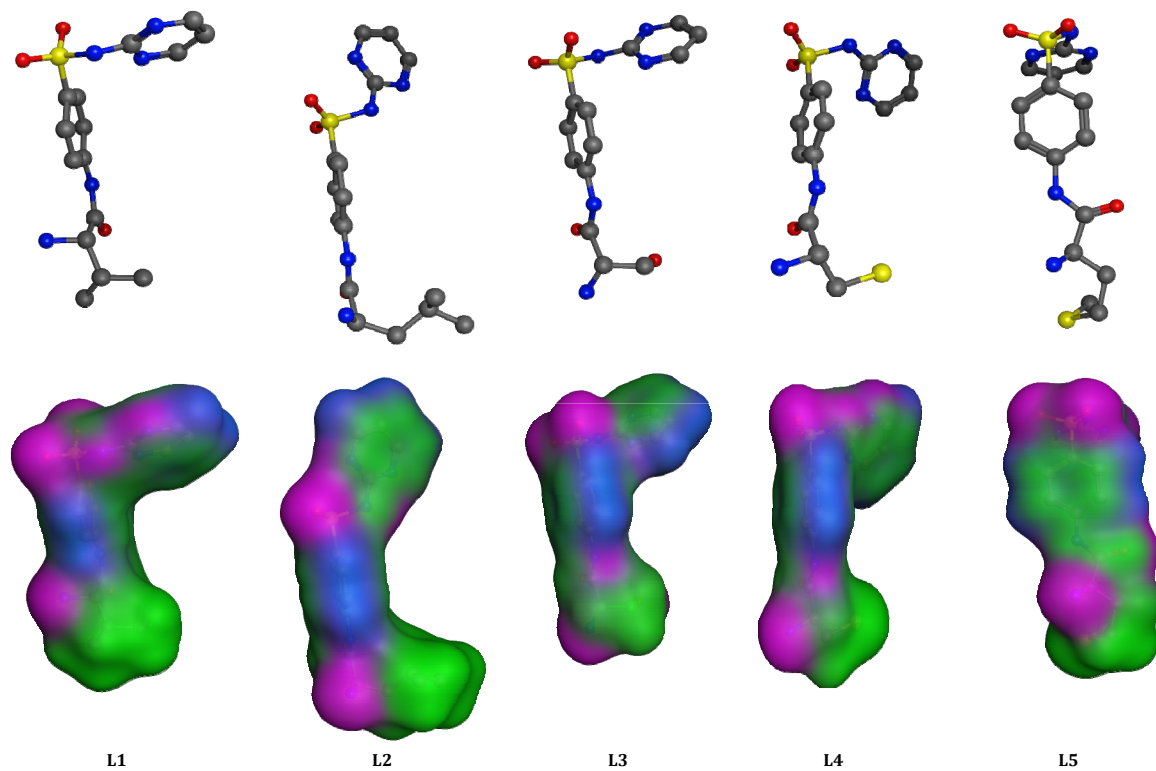


Figure 4. a) Minimal energy conformation, b) Electrostatic potential map of the prepared ligands (L1) VS, (L2) LS, (L3) SS, (L4) CS, (L5) MS. The position is slightly altered in (b) to allow a better view of the parameters analyzed.

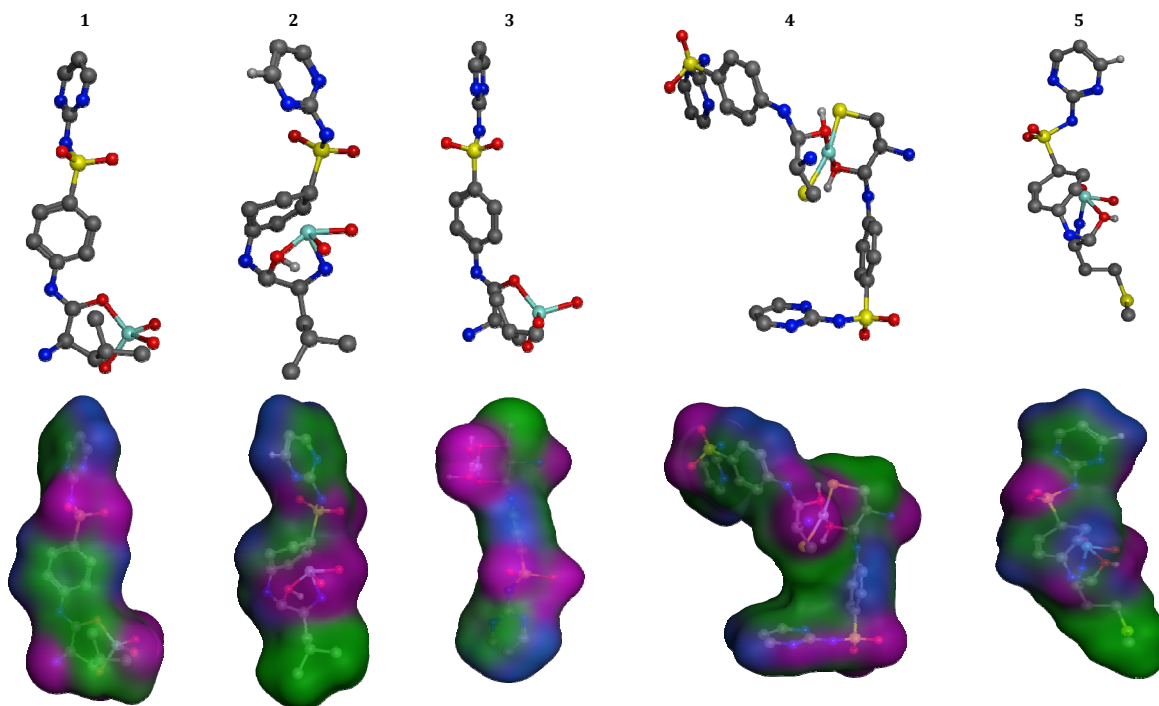


Figure 5. a) Minimal energy conformation, b) Electrostatic potential map of the prepared complexes (1) Zn^{II}-VS, (2) Zn^{II}-LS, (3) Zn^{II}-SS, (4) Zn^{II}-CS, (5) Zn^{II}-MS. The position is slightly altered in (b) to allow a better view of the parameters analyzed.

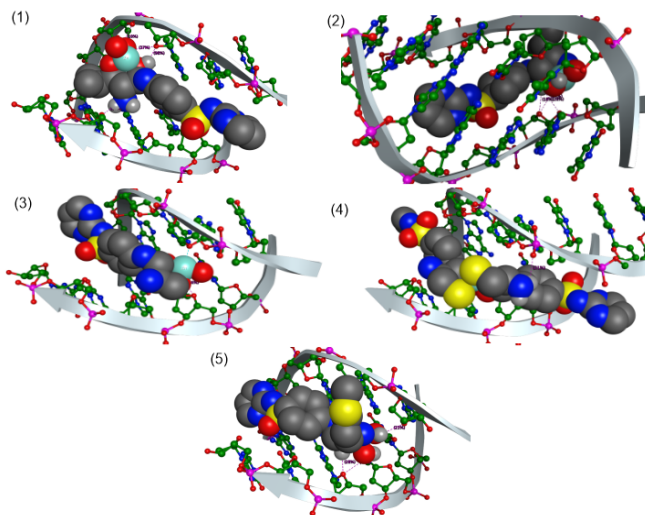


Figure 6. A predicted docking pose for the prepared Zn complexes (1) Zn^{II}-VS, (2) Zn^{II}-LS, (3) Zn^{II}-SS, (4) Zn^{II}-CS, (5) Zn^{II}-MS with [d(CGCAAATTTGCG)]₂ strands of DNA by minor groove binding approach.

Increasing HOMO energy and decreasing LUMO energy in the drug molecule lead to enhancement of stabilizing interactions, and hence, binding with the receptor.

Table 3 and 5 showed that the ligands (SS and CS) and their complexes (Zn^{II}-SS and Zn^{II}-CS) represented the lowest energy gap -8.74, -8.87, -8.85 and -5.75 eV, respectively. The three dimensional structure and the electrostatic potential map (Figure 4 and 5) were analyzed to identify the relation between the biological efficiency of the prepared compounds and their sizes, shapes and superficial charge distribution. The data showed that the substitution at α -carbon atom of amino acid with hydrogen bond donor groups (OH and SH) is playing an important role in increasing DNA binding affinity and antimicrobial activity.

3.6.3. Docking studies

In order to understand the binding mode of DNA-complex interactions, the docking study of our complexes were carried out. Docking experiment was performed using default parameters with MOE [55]. The crystal structure of [d(CGCAAATTTGCG)]₂ with distamycin (PDB ID: 2DND) was obtained from protein data bank PDB [60]. Distamycin was removed from the crystal structure before DOCKING experiment. The predicted top-ranking pose with lowest energy of complexes, was applied to suggesting the best possible geometry of the complexes inside the DNA double helix (Table 3, Figure 6). All docked complexes were represented in CPK to clarify the binding mode of these complexes with DNA. The preferred binding mode of the synthesized complexes in the target crystal structure is shown in Figure 6. Also, the current ligand-receptor interactions were analyzed on the basis of energy scores as described in (Table 3). The data obtained from analysis of the docked structures showed that;

- i. The metal complexes were stabilized by one or more H-bonds with the DNA bases,
- ii. All complexes stabilized themselves in the binding pocket by adjusting: (a) phenyl in plane with diazine ring in complexes Zn^{II}-VS and Zn^{II}-CS, (b) diazine coplanar with phenyl ring in complexes Zn^{II}-SS and Zn^{II}-MS, (c) diazine perpendicular with phenyl ring in Zn^{II}-LS,
- iii. At the same time the whole complexes were stabilized in the binding pocket base by adjusting

their phenyl and diazine rings parallel with DNA base in Zn^{II}-VS, Zn^{II}-CS and Zn^{II}-MS, but in case of Zn^{II}-LS and Zn^{II}-SS diazine rings were perpendicular with DNA base,

- iv. The complexes Zn^{II}-SS, Zn^{II}-CS and Zn^{II}-MS showed lowest docking energies pose -16.86, -18.83 and -16.50 kcal/mol, respectively and highest affinity (IC₅₀ = 10, 13 and 19 μ g/mL) for DNA (Table 3). The complexes Zn^{II}-VS and Zn^{II}-LS showed moderate affinity with docking energies between -14.30 and -4.11 kcal/mol.

4. Conclusion

Series of Zn(II) complexes have been prepared and characterized using physicochemical methods such as IR, electronic, and NMR spectroscopy. The activation parameters were determined by thermal analyses calculations. The prepared organic compounds behave as bidentate ligands. The binding of Zn(II) complexes as small molecules to DNA showed that the complexes Zn^{II}-SS, Zn^{II}-CS and Zn^{II}-MS revealed the highest binding affinity with the lowest docking energies pose. This efficiency of the binding mode may be due to existence polarity nature of the amino acid moiety. All ligands and Zn(II) complexes have been checked for antibacterial and antifungal activities. All synthesized ligands in this study showed a good oral absorption as antimicrobial compounds. These observations suggest that the antibiotic sulfadiazine can be modified using different amino acids for effective medication in the future.

Acknowledgement

The authors acknowledge Taif University for supporting this work by Taif University research program.

References

- [1]. Song, Y. M.; Wu, Q.; Yang, P. J.; Luan, N. N.; Wang, L. F.; Liu, Y. M. *J. Inorg. Biochem.* **2006**, *100*, 1685-1691.
- [2]. Tan, C. P.; Liu, J.; Chen, L. M.; Shi, S.; Ji, L. N. *J. Inorg. Biochem.* **2008**, *102*, 1644-1653.
- [3]. Zuber, G.; Quada Jr J. C.; Hecht, S. M. *J. Am. Chem. Soc.* **1998**, *120*, 9368-9396.
- [4]. Hecht, S. M. *J. Nat. Prod.* **2000**, *63*, 158-168.
- [5]. Lerman, L. S. *J. Mol. Biol.* **1961**, *3*, 18-30.

- [6]. Jonathan, B. C. *Biopolymers* **1997**, *44*, 201-215.
- [7]. Alessio, E. *Bioinorganic Medicinal Chemistry*, Wiley-VCH, Weinheim, 2011.
- [8]. Keene, F. R.; Smith, J. A.; Collins, J. G. *Coord. Chem. Rev.* **2009**, *253*, 2021-2035.
- [9]. Ott, I. *Coord. Chem. Rev.* **2009**, *253*, 1670-1681.
- [10]. Thurston, D. E., *Chemistry and Pharmacology of Anticancer Drugs*, CRC Press, Boca Raton, FL, 2007.
- [11]. Mederos, A.; Dominguez, S.; Hernandez-Molina, R.; Sanchiz, J.; Brito, F. *Coord. Chem. Rev.* **1999**, *857*, 193-195.
- [12]. Hambley, T. W. *Dalton Trans.* **2007**, *43*, 4929-4937.
- [13]. Han Ang, W.; Dyson, P. J. *Eur. J. Inorg. Chem.* **2006**, 4003-4018.
- [14]. Busto, N.; Valladolid, J.; Aliende, C.; Jalon, F. A.; Manzano, B. R.; Rodriguez, A. M.; Gaspar, J. F.; Martins, C.; Biver, T.; Espino, G.; Leal, J. M.; Garcia, B. *Chem. Asian J.* **2012**, *7*, 788-801.
- [15]. Al-Mogren, M. M.; Alaghaz, A. M. A.; Ebrahim, A. E. *Spectrochim. Acta A* **2013**, *114*, 695-707.
- [16]. Pothiraj, K.; Baskaran, T.; Raman, N. J. *Coord. Chem.* **2012**, *65*, 2110-2126.
- [17]. Holder, A. A. *Annu. Rep. Prog. Chem. Sect. A: Inorg. Chem.* **2012**, *108*, 350-368.
- [18]. Ronconi, L.; Sadler, P. J. *Coord. Chem. Rev.* **2007**, *251*, 1633-1648.
- [19]. Schwietert, C. W.; McCue, J. P. *Coord. Chem. Rev.* **1999**, *184*, 67-89.
- [20]. Vaira, M. D.; Bazzicalupi, C.; Orioli, P.; Messori, L.; Bruni, B.; Zatta, P. *Inorg. Chem.* **2004**, *43*, 3795-3797.
- [21]. Li, Z. Q.; Wu, F. J.; Gong, Y.; Hu, C. W.; Zhang, Y. H.; Gan, M. Y. *Chin. J. Chem.* **2007**, *25* 1809-1814.
- [22]. Sakurai, H.; Kojima, Y.; Yoshikawa, Y.; Kawabe, K.; Yasui, H. *Coord. Chem. Rev.* **2002**, *226*, 187-198.
- [23]. Zhou, Q.; Hambley, T. W.; Kennedy, B. J.; Lay, P. A.; Turner, P.; Warwick, B.; Biffin, J. R.; Regtop, H. L. *Inorg. Chem.* **2000**, *39*, 3742-3748.
- [24]. Kasuga, N. C.; Sekino, K.; Ishikawa, M.; Honda, A.; Yokoyama, M.; Nakano, S.; Shimada, N.; Koumo, C.; Nomiya, K. *J. Inorg. Biochem.* **2003**, *96*, 298-310.
- [25]. Travnicek, Z.; Krystof, V.; Sipl, M. J. *Inorg. Biochem.* **2006**, *100*, 214-225.
- [26]. Casas, J. S.; Castellano, E. E.; Couce, M. D.; Ellena, J.; Sanchez, A.; Sordo, J.; Taboada, C. J. *Inorg. Biochem.* **2006**, *100*, 124-132.
- [27]. You, Z. L.; Shi, D. H.; Xu, C.; Zhang, Q.; Zhu, H. L. *Eur. J. Med. Chem.* **2008**, *43*, 862-871.
- [28]. Mumih, P.; Moulin, A.; Stamper, C. C.; Bennett, B.; Ringe, D.; Petsko, G. A.; Holz, R. C. J. *Inorg. Biochem.* **2007**, *101*, 1099-1107.
- [29]. Zhang, H.; Liu, C. S.; Bu, X. H.; Yang, M. J. *Inorg. Biochem.* **2005**, *99*, 1119-1125.
- [30]. Sheng, X.; Guo, X.; Lu, X. M.; Lu, G. Y.; Shao, Y.; Liu, F.; Xu, Q. *Bioconjug. Chem.* **2008**, *19*, 490-498.
- [31]. Reedijk, J. in: Wilkinson, G.; Gillard, R. D.; McCleverty J. A. (Eds.), *Heterocyclic Nitrogen-Donor Ligands Comprehensive Coordination Chemistry*, vol. 2, Pergamon Press, Oxford, 1987, pp. 73.
- [32]. House, D. A.; in: Wilkinson, G.; Gillard, R. D.; McCleverty, J. A. (Eds.), *Ammonia and Amines. Comprehensive Coordination Chemistry*, vol. 2, Pergamon Press, Oxford, 1987, pp. 23.
- [33]. Grob, F.; Müller-Hartmann, A.; Vahrenkamp, H. *Eur. J. Inorg. Chem.* **2000**, *11*, 2363-2370.
- [34]. Wang, S. X.; Luo, Q. H.; Wang, X. M.; Wang, L. F.; Yu, K. B. *J. Chem. Soc. Dalton. Trans.* **1995**, *12*, 2045-2055.
- [35]. Pezzuto, J.; Che, C.; McPherson, D.; Zhu, P.; Topcu, G.; Erdelmeier, C.; Cordell, G. J. *Nat. Prod.* **1991**, *54*, 1522-1530.
- [36]. Burres, N.; Frigo, A.; Rasmussen, R.; McAlpine, J. J. *Nat. Prod.* **1992**, *55*, 1582-1597.
- [37]. Muanza, D.; Kim, B.; Euler, K.; Williams, L. *Pharm. Biol.* **1994**, *32*, 337-345.
- [38]. Irobi, O.; Moo-Young, M.; Anderson, W. *Pharm. Biol.* **1996**, *34*, 87-90.
- [39]. Wunsch, E.; Jaeger, E.; Kislafudy, L.; Low, M. *Angew. Chem.* **1977**, *16*, 317-318.
- [40]. Hanafy, A. I.; El-Bahy, Z. M.; Ali, I. O. J. *Coord. Chem.* **2012**, *65*, 1459-1474.
- [41]. Mostafa, H. Y. J. *Pigm. Resin. Res. Tech.* **2006**, *35*, 71-75.
- [42]. Selvam, P.; Rathore, P.; Karthikumar, S.; Velkumar, K.; Palanisamy, P.; Vijayalakshmi, S.; Witvrouw, M. *Ind. J. Pharm. Sci.* **2009**, *71*, 432-436.
- [43]. Majumder, A.; Rosair, G. M.; Mallick, A.; Chattopadhyay, N.; Mitra, S. *Polyhedron* **2006**, *25*, 1753-1762.
- [44]. Lever, A. B. P. *Inorganic Electronic Spectroscopy*, Elsevier, Amsterdam, 1984.
- [45]. Osowole, A. A.; Kolawole, G. A.; Fagade, O. E. *Synth. React. Inorg. Met. Org. Chem. Nano-Met. Chem.* **2005**, *35*, 829-836.
- [46]. Coats, A. W.; Redfern, J. P. *Nature* **1964**, *201*, 68-69.
- [47]. Hanafya, A. I.; El-Bahy, Z. M.; El-Henawy, A. A.; Faheim, A. A. J. *Mol. Catal. A* **2012**, *355*, 192-200.
- [48]. Mohameda, G. G.; Sharaby, C. M. *Spectrochim. Acta Part A* **2007**, *66*, 949-958.
- [49]. Singh, B. K.; Mishra, P.; Garg, B. S. *Spectrochim. Acta Part A* **2008**, *69*, 361-370.
- [50]. El-Bendary, E.; El-Sherbeny, M.; Badria, F. *Boll. Chim. Farmaceutico* **1998**, *137*, 115-119.
- [51]. El-Bendary, E.; Badria, F. *Arch. Pharm. Med. Chem.* **2000**, *333*, 99-103.
- [52]. Zhao, Y.; Abraham, M. H.; Lee, J.; Hersey, A.; Luscombe, N. C.; Beck, G.; Sherborne, B.; Cooper, I. *Pharm. Res.* **2002**, *19*, 1446-1457.
- [53]. Lipinski, C. A.; Lombardo, F.; Dominy, B. W.; Feeney, P. J. *Adv. Drug. Delivery Rev.* **1997**, *23*, 3-25.
- [54]. Clark, D. E.; Pickett, S. D. *Drug Discov. Today* **2000**, *5*, 49-58.
- [55]. Molecular Operating Environment (MOE), 2009.10; Chemical Computing Group Inc., Montreal, QC, Canada.
- [56]. Wildman, S. A.; Crippen, G. M. *J. Chem. Inf. Comput. Sci.* **1999**, *39*, 868-873.
- [57]. Profeta, S.; Allinger, N. L. *J. Am. Chem. Soc.* **1985**, *107*, 1907-1918.
- [58]. Halgren, T. A. *J. Comput. Chem.* **1996**, *17*, 490-519.
- [59]. Dewar, M. J. S.; Zoebisch, E. G.; Healy, E. F.; Stewart, J. J. P. *J. Am. Chem. Soc.* **1985**, *107*, 3902-3909.
- [60]. Fukui, K. *Science* **1982**, *218*, 747-754.